

Clustering properties of a sterile neutrino dark matter candidate.

D. Boyanovsky*

Department of Physics and Astronomy, University of Pittsburgh, Pittsburgh, Pennsylvania 15260, USA.

(Dated: October 26, 2018)

The clustering properties of sterile neutrinos are studied within a simple extension of the minimal standard model, where these neutrinos are produced via the decay of a gauge singlet scalar. The distribution function after decoupling is strongly out of equilibrium and features an enhancement at small comoving momentum $\propto 1/\sqrt{p}$. Dark matter abundance and phase space density constraints from dwarf spheroidal galaxies constrain the mass in the keV range consistent with a Yukawa coupling to a gauge singlet with mass and vacuum expectation value in the range ~ 100 GeV and a decoupling temperature of this order. The dark matter transfer function and power spectrum are obtained from the solution of the non-relativistic Boltzmann-Vlasov equation in the matter dominated era. The small momentum enhancement of the non-equilibrium distribution function leads to long range memory of gravitational clustering and a *substantial enhancement of the power spectrum at small scales as compared to a thermal relic or sterile neutrino produced via non-resonant mixing with active neutrinos*. The scale of suppression of the power spectrum for a sterile neutrino with $m \sim \text{keV}$ produced by scalar decay that decouples at $\sim 100\text{GeV}$ is $\lambda \sim 488 \text{ kpc}$. At large scales $T(k) \sim 1 - C k^2/k_{fs}^2(t_{eq}) + \dots$ with $C \sim \mathcal{O}(1)$. At small scales $65 \text{ kpc} \lesssim \lambda \lesssim 500 \text{ kpc}$ corrections to the fluid description and memory of gravitational clustering become important, and we find $T(k) \simeq 1.902 e^{-k/k_{fs}(t_{eq})}$, where $k_{fs}(t_{eq}) \sim 0.013/\text{kpc}$ is the free streaming wavevector at matter-radiation equality. The enhancement of power at small scales may provide a possible relief to the tension between the constraints from X-ray and Lyman- α forest data.

I. INTRODUCTION

In the *concordance* ΛCDM standard cosmological model dark matter (DM) is composed of primordial particles which are cold and collisionless[1]. In this cold dark matter (CDM) scenario structure formation proceeds in a hierarchical “bottom up” approach: small scales become non-linear and collapse first and their merger and accretion leads to structure on larger scales. CDM particles feature negligible small velocity dispersion leading to a power spectrum that favors small scales. In this hierarchical scenario, dense clumps that survive the merger process form satellite galaxies.

Large scale simulations seemingly yield an overprediction of satellite galaxies[2] by almost an order of magnitude larger than the number of satellites that have been observed in Milky-Way sized galaxies[2, 3, 4, 5, 6]. Simulations within the ΛCDM paradigm also yield a density profile in virialized (DM) halos that increases monotonically towards the center[2, 7, 8, 9, 10] and features a cusp, such as the Navarro-Frenk-White (NFW) profile[7] or more general central density profiles $\rho(r) \sim r^{-\beta}$ with $1 \leq \beta \lesssim 1.5$ [4, 7, 10]. These density profiles accurately describe clusters of galaxies but there is an accumulating body of observational evidence[11, 12, 13, 14, 15, 16, 18, 19] that seem to indicate that the central regions of (DM)-dominated dwarf spheroidal satellite (dSphs) galaxies feature smooth cores instead of cusps as predicted by (CDM). More recently[19] a “galaxy size” problem has been reported, where large scale simulations at $z = 3$ yield galaxies that are too small, this problem has been argued to be related to that of the missing dwarf galaxies.

Warm dark matter (WDM) particles were invoked[20, 21, 22] as possible solutions to these discrepancies both in the over abundance of satellite galaxies and as a mechanism to smooth out the cusped density profiles predicted by (CDM) simulations into the cored profiles that fit the observations in (dShps). (WDM) particles feature a range of velocity dispersion in between the (CDM) and hot dark matter (HDM) leading to free streaming scales that smooth out small scale features and could be consistent with core radii of the (dSphs). If the free streaming scale of these particles is smaller than the scale of galaxy clusters, their large scale structure properties are indistinguishable from (CDM) but may affect the *small* scale power spectrum[23] so as to provide an explanation of the smoother inner profiles of (dSphs), fewer satellites and the size of galaxies at $z = 3$ [19].

Sterile neutrinos with masses $\sim \text{keV}$ may be suitable (WDM) candidates[24, 26, 27, 28, 29, 30]. The main property that is relevant for structure formation of any dark matter candidate is its distribution function after decoupling[32, 33], which depends on the production mechanism and the (quantum) kinetics of its evolution from production to

*Electronic address: boyan@pitt.edu

decoupling. There is a variety of mechanisms of sterile neutrino production[24, 25, 26, 27, 34], and mixing between sterile and active neutrinos can be one of them[24, 25, 26]. There is considerable tension between the X-ray[35] and Lyman- α forest[36, 37] data if sterile neutrinos are produced via the Dodelson-Widrow (DW)[24] non-resonant mixing mechanism, leading to the suggestion[38] that these cannot be the dominant (DM) component. Constraints from the Lyman- α forest spectra are particularly important because of its sensitivity to the suppression of the power spectrum by free-streaming in the linear regime[36, 37]. The most recent constraints from the Lyman- α forest[37] improve upon previous ones, but rely on the Dodelson-Widrow[24] model for the distribution function of sterile neutrinos, leaving open the possibility of evading these tight constraints with non-equilibrium distribution functions from other production mechanisms.

The gravitational clustering properties of collisionless (DM) in the linear regime are described by the power spectrum of gravitational perturbations. Free streaming of collisionless (DM) leads to a suppression of the transfer function on length scales smaller than the free streaming scale via Landau damping[23, 39, 40]. This scale is determined by the decoupling temperature, the particle’s mass and the distribution function at decoupling[41].

In this article we study the gravitational clustering properties of sterile neutrinos as (WDM) candidates within a model in which these are produced via the decay of a gauge singlet scalar. Such model has been advocated recently in ref.[29, 30, 34], and is based on a phenomenologically appealing extension of the minimal standard model[27] consistent with the observed neutrino masses and mixing. This model also shares many features in common with models of gravitino production[42], hence it provides a viable extension of the standard model to study in detail the production and clustering properties of potential (WDM) candidates. In this model sterile neutrinos decouple at temperatures much larger (~ 100 GeV) than in the Dodelson-Widrow scenario (~ 150 MeV)[24], therefore they are *colder* at matter-radiation equality (and today), being dubbed, for this reason, “chilled” neutrinos in refs.[29, 30]. Clustering properties of active neutrinos in non-standard cosmology, for example quintessence have been reported in ref.[31].

A program that yields a quantitative assessment of a particle physics candidate for (DM) in the linear regime implements the following steps:

- Establish the quantum kinetic equations that describe the production of these particles and follows the evolution of their distribution function through their decoupling from the cosmological plasma.
- The distribution function after decoupling becomes the *unperturbed* distribution, which determines the abundance, the primordial phase space densities[32, 33] and free streaming lengths[41]. The generalized Tremaine-Gunn[43] constraints obtained in[33] in combination with the recent photometric observations of the phase space densities of (dSphs) combined with the DM abundance lead to bounds on the mass, couplings and decoupling temperature[33].
- The unperturbed distribution function is input in the Boltzmann-Vlasov equation for density and gravitational perturbations[44]. The solution of which yields the transfer function, and the power spectrum.

We follow this program in the model of sterile neutrino production proposed in refs.[27, 29, 30, 34]. In principle, in order to obtain the transfer function and the power spectrum of density perturbations the coupled set of Boltzmann equations for baryons, photons, dark matter and gravitational perturbations must be solved[44, 45]. Photons and baryons are coupled by Thompson scattering and dark matter only couples to the gravitational perturbations that are sourced by all the components. In practice this is a computationally daunting task because popular codes[46] based on the set of coupled Boltzmann equations for photons, baryons and dark matter[44] need to be modified to input arbitrary non-equilibrium distribution functions, masses and couplings.

Recently a simple analytic framework to obtain the dark matter transfer function, and consequently the power spectrum during matter domination has been presented[47]. The main premise of this formulation is that the contribution from baryons and photons modifies the DM transfer function at most by a few percent[48, 49] during matter domination and that a preliminary robust assessment of the clustering properties of a DM candidate can be systematically established by neglecting in first approximation the contribution from baryons and photons. The influence of baryons on the DM power spectrum is more prominent on the scale of baryon acoustic oscillations (BAO), corresponding to the scale of the sound horizon at recombination, or ~ 150 Mpc today[50]. On this scale the DM power spectrum does not distinguish between (CDM) or (WDM), and at smaller scales, of interest for the satellite and cusp problems, the (BAO) features are not prominent and can be safely neglected.

The main ingredient to study the (DM) transfer function in absence of baryons is the non-relativistic Boltzmann-Vlasov equation for DM density and gravitational perturbations. The non-relativistic limit is warranted for particles that decoupled early and became non-relativistic prior to matter-radiation equality and for perturbations that entered the horizon prior to matter-radiation equality, these describe all the relevant scales for structure formation.

The method developed in ref.[47] yields a simple analytic approximation to the transfer function that is remarkably accurate in a wide range of scales relevant to structure formation. An important ingredient is a non-local kernel that

depends on the unperturbed distribution function of the decoupled particles. This kernel describes memory of gravitational clustering and is a *correction to the fluid description* which become important at small scales. Distribution functions that feature larger support at small momentum yield longer range memory kernels thereby enhancing the transfer function at small scales[47]placing greater importance on non-equilibrium aspects of the distribution function.

In this article we study the clustering properties of sterile neutrinos in the model proposed in references[27, 29, 30, 34] by implementing all the steps described above, from obtaining and solving the quantum kinetic equation for production that establishes the distribution function at decoupling, narrowing the range of parameters, masses and couplings with the observational constraints from (DM) abundance and coarse grained phase space densities of (DM) dominated (dSphs)[14, 33], and solving the Boltzmann-Vlasov equation obtaining the transfer function and power spectrum which we compare to the case of thermal relics or Dodelson-Widrow-type[24] distribution functions.

Summary of results:

The production of sterile neutrinos of $m \sim \text{keV}$ via the decay of scalar gauge singlet with $M \sim 100 \text{ GeV}$ leads to decoupling at a temperature $\sim 100 \text{ GeV}$ and a distribution function that is strongly out of equilibrium and behaves as $1/\sqrt{p}$ for small comoving momenta p .

The constraints from (DM) abundance and coarse-grained phase space density from the latest compilation of photometric data from (dSphs) lead to a narrow window in the keV range for the value of the mass of the sterile neutrino, consistently with the phenomenologically motivated extension beyond the standard model studied.

The (DM) transfer function and power spectrum are obtained from the solution of the non-relativistic Boltzmann-Vlasov equation for (DM) density and gravitational perturbations during matter domination. We implement a simple analytic approximate method[47] to obtain the density and gravitational perturbations and the transfer function that is remarkably accurate in a wide range of cosmologically relevant scales, as confirmed by the exact solution. This approach yields a wealth of information that relates the small scale behavior of the transfer function to the range of memory of gravitational clustering, which is determined by the small (comoving) momentum region of the distribution function.

The enhancement of the non-equilibrium distribution at small momentum leads to a long range memory of gravitational clustering and slower fall off of the free-streaming solution. Both features lead to an enhancement of the transfer function and power spectrum at small scales.

We compare the transfer function and power spectrum from sterile neutrinos produced via gauge singlet decay to that of relativistic fermions decoupled in local thermodynamic equilibrium (LTE) (thermal relic) and sterile neutrinos produced by non-resonant mixing with active neutrinos *a la* Dodelson-Widrow[24]. Thermal relics and (DW)-produced sterile neutrinos feature the *same* transfer function for similar ratios of the decoupling temperature to mass.

The transfer function and power spectrum for sterile neutrinos produced by scalar decay is *substantially enhanced* with respect to that of (DW)-sterile neutrinos (and thermal relics) at small scales $\lambda \lesssim 500 \text{ kpc}$. Whereas for (DW)-sterile neutrinos with $m \sim \text{keV}$ the transfer function is suppressed on scales $\lambda \lesssim 900 \text{ kpc}$, the scale of suppression for $m \sim \text{keV}$ sterile neutrinos produced by scalar decay at a scale $\sim 100 \text{ GeV}$ is $\lambda \lesssim 488 \text{ kpc}$ with a large enhancement of power at smaller scales.

For sterile neutrinos produced by scalar decay we find the following behavior for the transfer function: at long wavelengths,

$$T(k) \simeq 1 - C \left(\frac{k}{k_{fs}(t_{eq})} \right)^2 + \dots \quad ; \quad k \ll k_{fs}(t_{eq}) \quad (1.1)$$

with $C \sim \mathcal{O}(1)$, and at small scales where the corrections to the fluid description and the memory of gravitational clustering becomes important

$$T(k) \simeq 1.902 e^{-k/k_{fs}(t_{eq})} \quad ; \quad k \geq k_{fs}(t_{eq}) \quad (1.2)$$

valid for scales $65 \text{ kpc} \lesssim \lambda \lesssim 500 \text{ kpc}$ where $k_{fs}(t_{eq})$ is the free streaming wavevector at matter radiation equality. For $m \sim \text{keV}$ and decoupling temperature $\sim 100 \text{ GeV}$ we obtain $k_{fs}(t_{eq}) \sim 0.013/\text{kpc}$.

The smaller suppression scale may relieve the tension between the X-ray[35] and Lyman- α forest[36, 37] data and may provide the necessary enhancement of power at small scales to smooth out the inner profile of (dSphs).

II. THE MODEL

We study the model presented in references[27, 29, 30, 34] as an extension of the minimal standard model with only one sterile neutrino, however, including more species is straightforward. The Lagrangian density is given by

$$\mathcal{L} = \mathcal{L}_{SM} + \frac{1}{2}\partial_\mu\chi\partial^\mu\chi - \frac{M^2}{2}\chi^2 + i\bar{\nu}\not{\partial}\nu - \frac{Y}{2}\chi\bar{\nu}^c\nu - \frac{m}{2}\bar{\nu}^c\nu - y_\alpha H^\dagger\bar{L}_\alpha\nu - V(H^\dagger H; \chi) + \text{h.c.} \quad (2.1)$$

where \mathcal{L}_{SM} is the standard model Lagrangian, $L_\alpha; \alpha = 1, 2, 3$ are the standard model $SU(2)$ lepton doublets, ν is a singlet sterile neutrino with a (Majorana) mass m , a real scalar χ with Yukawa coupling Y to the sterile neutrino which in turn is Yukawa coupled to the active neutrinos via the Higgs doublet H , thereby building a see-saw mass matrix in terms of the vacuum expectation of this doublet[27, 29, 34].

As discussed in detail in ref.[33] abundance and phase space density constraints from (d)Sphs indicate that the mass of suitable (WDM) candidates must be in the keV range, which leads to considering the vacuum expectation value and mass M of the singlet scalar χ in the range ~ 100 GeV as discussed in references[29, 30, 34]. If the sterile neutrino mass $m \sim \text{keV}$ results from the vacuum expectation value $\langle\chi\rangle \sim 100$ GeV then the Yukawa coupling $Y \sim 10^{-8}$.

The results of the study here demonstrate that this range of parameters yields a consistent description of sterile neutrinos as a suitable (DM) candidate in this model.

A. Decoupling out of equilibrium

Non-resonant active-sterile mixing leads to sterile neutrino production via the Dodelson-Widrow mechanism[24] with a decoupling temperature near the QCD scale[24, 26] ~ 150 MeV. In this scenario the distribution function at decoupling is of the form[24]

$$f_{dw}(P_f; T) = \frac{\beta}{e^y + 1} \quad ; \quad y = \frac{P_f}{T} \quad ; \quad 0 < \beta \leq 1 \quad (2.2)$$

where P_f is the physical momentum. For sterile neutrinos produced by non-resonant mixing with active neutrinos[24] $\beta \propto \theta_m^2$ where $\theta_m \lesssim 10^{-2}$ [26, 35] is the mixing angle. A fermionic relic decoupled in local thermodynamic equilibrium (LTE) while relativistic corresponds to $\beta = 1$. This general type of distribution function with a suppression factor β has been used in the Lyman- α forest analysis[37].

In this article we will neglect this production mechanism and focus on the production via the decay of the gauge singlet scalar field χ which, as discussed in references[29, 30, 34] lead to ‘‘colder’’ relics. However, we will compare the clustering properties of the distribution obtained via this mechanism and that of relics that decoupled with the generalized distributions (2.2), postponing to another study the complete kinetic description that accounts for both processes. Since these production mechanisms are effective at widely different scales (~ 100 GeV for $\chi \rightarrow \bar{\nu}\nu$ -decay[29, 30, 34], vs. ~ 150 MeV for Dodelson-Widrow[24, 26]) we expect that possible corrections from mixing will be subleading and certainly so for the small y region of interest. A more complete study is forthcoming.

We consider the case in which the Yukawa coupling $Y \ll 1$ and $M \gg m$ and assume that the scalar field χ is strongly coupled to the plasma and is in (LTE) with a Bose-Einstein distribution function¹

$$N_k = \frac{1}{e^{\Omega_k(t)/T(t)} - 1} \quad ; \quad \Omega_k(t) = \sqrt{\frac{k^2}{a^2(t)} + M^2} \quad (2.3)$$

where k is a comoving wavevector and

$$T(t) = \frac{T_0}{a(t)} \quad (2.4)$$

where T_0 would be the temperature of the plasma *today*. During the radiation dominated era the Hubble expansion rate is given by[40]

$$H(t) \simeq 1.66g^{\frac{1}{2}}(t)\frac{T^2(t)}{M_{pl}} \quad (2.5)$$

where $g(t)$ is the effective number of relativistic degrees of freedom.

¹ The case where the scalar is out of equilibrium has been considered in[29, 30].

The details leading to the quantum kinetic equation for the production of sterile neutrinos via the decay of the scalar field χ are given in the appendix and the final result is given by eqn. (A8).

For $Y^2 \ll 1$ we expect that neutrinos will decouple early and their distribution function will freeze-out with $n_p, \bar{n}_p \ll 1$. This expectation will be confirmed below self-consistently from the solution of the kinetic equation. Neglecting the neutrino population buildup in the kinetic equation (A8), namely setting $n_p = \bar{n}_q = 0$, neglecting terms of order $m^2/M^2 \ll 1$, taking the scalar field to be in LTE and replacing the momenta in (A8) by their physical values, we find from (A8)

$$\frac{dn(p; t)}{dt} = \frac{Y^2 M^2 T(t)}{8\pi P_f(t) \omega_p(t)} \ln \left[\frac{1 - e^{-(\omega_+(t) + \omega_p(t))/T(t)}}{1 - e^{-(\omega_-(t) + \omega_p(t))/T(t)}} \right] \quad (2.6)$$

where $P_f(t) = p/a(t)$ is the physical momentum, p is the comoving momentum and

$$\omega_p(t) = \sqrt{\frac{p^2}{a^2(t)} + m^2} \quad (2.7)$$

$$\omega_{\pm}(t) = \sqrt{q_{\pm}^2(t) + m^2} \quad (2.8)$$

where $q_{\pm}(t)$ are given by eqn. (A9) in the appendix in terms of the corresponding physical momenta. These values are determined by the kinematic thresholds for scalar decay.

We anticipate self-consistently, that for $Y \ll 1$ neutrinos decouple at temperatures $T_d \gg m$, namely when they are still relativistic, therefore we can safely neglect terms of order $m^2/T^2(t) < m^2/T_d^2 \ll 1$. Under this assumption (to be confirmed self-consistently below), using $P_f(t)/T(t) = p/T_0$ and neglecting terms of order $m^2/M^2 \ll 1$, the kinetic equation above simplifies considerably. It proves convenient to use the dimensionless variables

$$\tau = \frac{M}{T(t)} \quad (2.9)$$

with

$$\frac{d\tau}{dt} = \tau H(t) \quad (2.10)$$

and

$$y = \frac{p}{T_0} \quad (2.11)$$

leading to the following form of the quantum kinetic equation,

$$\frac{dn(y; \tau)}{d\tau} = \Lambda(\tau) \left(\frac{\tau}{y}\right)^2 \ln \left[\frac{1 - e^{-M^2 y/m^2}}{1 - e^{-y - \tau^2/4y}} \right] \quad (2.12)$$

where we have introduced

$$\Lambda(\tau) = \frac{Y^2}{8\pi(1.66 g^{\frac{1}{2}}(t))} \left(\frac{M_{Pl}}{M}\right) \quad (2.13)$$

and the effective number of relativistic degrees of freedom depends on time through the temperature.

Under the assumption $M \gg m$, for example taking $M \sim 100$ GeV, $m \sim$ keV, the exponential in the numerator inside the logarithm can be neglected for all $y \gg m^2/M^2 \sim 10^{-16}$. Although we are interested in the small momentum region of the distribution function (small y), the phase space suppression for small momentum in the integrals of the distribution function entails that we can safely neglect the contributions of such small values of y . This argument will be confirmed explicitly below. Therefore we safely neglect the numerator inside the logarithm in (2.12). In order to integrate the rate equation (2.12) we must furnish $g(t)$. In the Standard Model this function is approximately constant in large intervals and features sharp variations in the regions of temperature when relativistic degrees of freedom either decay, annihilate or become non-relativistic[40].

We will *assume* that $g(t)$ is approximately constant in the region of (large) temperature before and during decoupling, replacing the value of g by its average \bar{g} over the range in which the rate (2.12) is appreciable. The numerical analysis presented below justifies this assumption for a wide range of y . Therefore we replace

$$\Lambda(\tau) \simeq \Lambda = \frac{Y^2}{8\pi(1.66 \bar{g}^{\frac{1}{2}})} \left(\frac{M_{Pl}}{M}\right). \quad (2.14)$$

With these approximations and assumptions, eqn. (2.12) is equivalent to the quantum kinetic equation obtained in references[27, 29, 42] and can be integrated exactly. We obtain,

$$n(y; \tau) = \Lambda \left\{ 2\sqrt{\pi} \frac{g_{\frac{5}{2}}(y)}{y^{\frac{1}{2}}} + \frac{\tau^3}{3y^2} \ln \left[\frac{1}{1 - e^{-y - \tau^2/4y}} \right] - \frac{8}{3y^2} \sum_{n=1}^{\infty} \frac{e^{-ny}}{n^{\frac{5}{2}}} \Gamma \left[\frac{5}{2}, \frac{n\tau^2}{4y} \right] \right\} \quad (2.15)$$

where²

$$g_{\frac{5}{2}}(y) = \sum_{n=1}^{\infty} \frac{e^{-ny}}{n^{\frac{5}{2}}} \quad ; \quad g_{\frac{5}{2}}(0) = \zeta \left(\frac{5}{2} \right) = 1.342 \dots \quad (2.16)$$

and $\Gamma[a, b]$ is the incomplete Gamma function.

The rate (2.12) vanishes as $\tau \rightarrow 0$, reaches a maximum and falls-off exponentially as $\tau/4y \rightarrow \infty$. The maximum rate is larger for *smaller* values of y , this feature translates into an *enhancement* of the distribution function at small momenta, which will be at the heart of the important aspects of clustering studied in section (IV).

The asymptotic behavior of the distribution function (2.15) for $\tau/4y \gg 1$ is given by

$$n(y; \tau) \stackrel{\tau^2/4y \gg 1}{\simeq} \Lambda \left[2\sqrt{\pi} \frac{g_{\frac{5}{2}}(y)}{y^{\frac{1}{2}}} + \frac{\tau^3}{3y^2} e^{-y} e^{-\tau^2/4y} - \frac{\tau^3}{3y^{\frac{7}{2}}} \sum_{n=1}^{\infty} \frac{e^{-ny} e^{-n\tau^2/4y}}{n} \right] \quad (2.17)$$

Figure (1) displays the rate (2.12) (left panel) and the distribution function (2.15) (right panel) as a function of τ for several values of y . For $y \ll 1$ the distribution function is largest, reaching its asymptotic value for $\tau \lesssim 1$, whereas for large values $y \gg 1$ the distribution function is strongly suppressed and reaches its asymptotic form much later (see fig.1).

Hence, for small y , the region of distribution function most relevant for small scale structure formation[47], decoupling occurs fairly fast, at a decoupling temperature $\sim M \gg m$ thus justifying the assumption of a constant $g(t)$ and $m/T_d \ll 1$ with $T_d = T_0$.

As discussed above and in ref.[47], the dark matter transfer function depends more sensitively on the *small* momentum (small y) region of the distribution function, the above analysis shows that for $y < 1$ the distribution function freezes out on a “time” scale $\tau \simeq 1$, namely a temperature scale $T(t_f) \sim M$, where t_f is the “freeze-out” time. Hence if the effective number of relativistic degrees of freedom $g(t)$ varies smoothly within the temperature range in which the population freezes-out $\sim M$ the approximation (2.14) is justified and reliable. Therefore we take the value \bar{g} as the effective number of relativistic degrees of freedom at decoupling, for example for a freeze-out temperature $T(t_f) \sim M \sim 100$ GeV in the standard model $\bar{g} \sim 100$ [40].

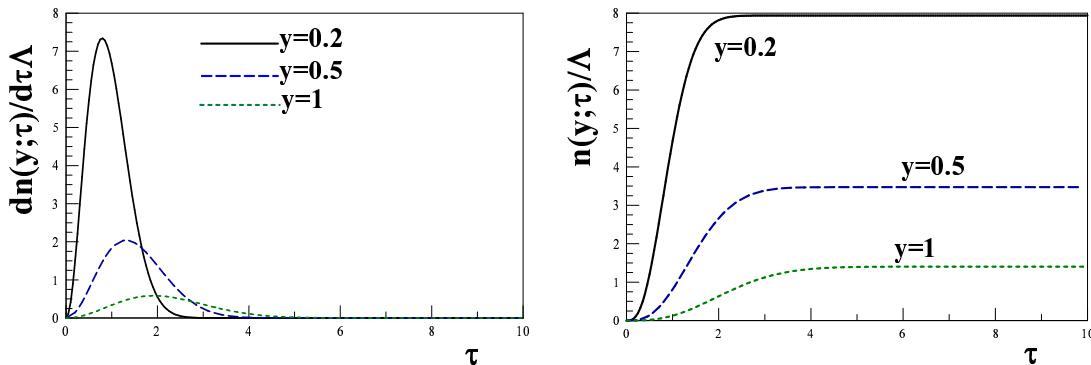


FIG. 1: Left panel: $dn(y; \tau)/d\tau \Lambda$ for $y = 0.2, 0.5, 1$. Right panel $n(y; \tau)/\Lambda$ for the same values of y .

The distribution function at freeze-out is obtained by taking the $\tau/4y \rightarrow \infty$ limit in eqn. (2.15), therefore we introduce the distribution function at decoupling

$$f_0(y) \equiv n(y; \infty) = 2\Lambda \sqrt{\pi} \frac{g_{\frac{5}{2}}(y)}{y^{\frac{1}{2}}}. \quad (2.18)$$

² Surprisingly the function $g_{\frac{5}{2}}(z)$ also determines the equation of state of the ideal non-relativistic Bose gas.

This is the *unperturbed* distribution function that enters in the Boltzmann-Vlasov equation that determines the evolution of density and gravitational perturbations, and is displayed in fig. (2). It is remarkable that for $y \ll 1$

$$f_0(y) \propto \frac{1}{y^{\frac{1}{2}}}, \quad (2.19)$$

in striking contrast to the thermal Fermi-Dirac distribution function and to the one obtained from the (DW) mechanism proposed in refs.[24, 25], and closer to that of a (non-condensed) bosonic massless particle for which the distribution function at small momentum is $\sim 1/y$.

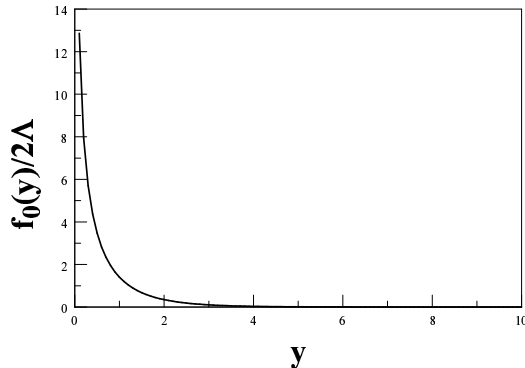


FIG. 2: The distribution function $f_0(y) = n(y; \infty)$.

The divergence of the distribution function $f_0(y)$ for $y \rightarrow 0$ must be interpreted with care because we have neglected the build-up of the neutrino population in the quantum kinetic equation, furthermore we have also neglected terms $\sim m/T(t_f) \sim m/M$ in the derivation. Neglecting the neutrino population in the kinetic equation requires that $f_0(y) \ll 1$ for all values of y , and neglecting the ratio $m/T(t_f)$ in the frequencies requires that $y \gg m/T(t_f) \sim m/M$. These constraints imply a range of couplings for which the approximations leading to the final result of the distribution function are reliable. For example, taking $m \sim \text{keV}$; $M \sim 100 \text{ GeV}$ neglecting the term $m/T(t_f) \sim m/M$ requires that $y \gg 10^{-8}$. To obtain an estimate of the range in which the population build-up can be neglected, it is convenient to write

$$\Lambda \simeq 3(Y \times 10^7)^2 \left(\frac{100}{\bar{g}} \right)^{\frac{1}{2}} \left(\frac{100 \text{ GeV}}{M} \right), \quad (2.20)$$

As discussed above (see also ref.[29, 34]) taking the expectation value of the scalar $\langle \chi \rangle \sim M \sim 100 \text{ GeV}$ and assuming that the neutrinos obtain their mass via the Yukawa coupling with $m \sim \text{keV}$, this implies $Y \sim 10^{-8}$ leading to the illustrative estimate $\Lambda \sim 0.03$. The condition for negligible neutrino population becomes

$$\frac{\Lambda}{y^{\frac{1}{2}}} \ll 1 \quad (2.21)$$

leading to $y \gg 10^{-4}$ for which we can safely ignore $m/T(t_f)$ and the build-up of the neutrino population. This constraint may be implemented by introducing an infrared cutoff $y_c \simeq 10^{-4}$ in the y - integrals of the distribution function, however, our analysis below shows that this is a mild constraint because of the phase space suppression in these integrals, hence the lower limit can be safely taken to $y = 0$. Values of $\bar{g} > 100$ and $M > 100 \text{ GeV}$ yield smaller values of Λ and larger region of reliability for y .

III. CONSTRAINTS FROM (DM) ABUNDANCE AND (DSPHS) PHASE SPACE DENSITY.

The number density *today* of this DM candidate is

$$n_0 = \frac{T_0^3}{2\pi^2} \int_0^\infty y^2 f_0(y) dy \quad (3.1)$$

where

$$\int_0^\infty y^2 f_0(y) dy = \frac{3\pi}{2} \Lambda \zeta(5) \quad ; \quad \zeta(5) = 1.037 \dots \quad (3.2)$$

Since this DM particle is non-relativistic today, its energy density is given by

$$\rho_{0M} = m n_0. \quad (3.3)$$

Entropy conservation[40] entails that

$$T_0 = \left(\frac{2}{g_d} \right)^{\frac{1}{3}} T_{cmb} \quad (3.4)$$

where $T_{cmb} = 2.348 \times 10^{-4}$ eV is the temperature of the cosmic microwave background today, and $g_d = \bar{g}$ is the effective number of relativistic degrees of freedom at decoupling.

The condition that this DM candidate contributes a fraction $0 \leq \nu_{DM} \leq 1$ to the (DM) density yields the following *upper* bound on the mass[33]

$$m \leq 2.695 \text{ eV} \frac{2\bar{g}\zeta(3)}{g \int_0^\infty y^2 f_0(y) dy} \lesssim 1.33 \left(\frac{\bar{g}}{g\Lambda} \right) \text{ eV}, \quad (3.5)$$

where g is the number of internal degrees of freedom of the particle. For a decoupling temperature ~ 100 GeV for which[40] $\bar{g} \sim 100$ and $\Lambda \sim 0.01 - 0.1$ this upper bound is in the keV range.

For comparison, for a fermion relic that decoupled with the general distribution function (2.2) the corresponding upper bound becomes

$$m \leq 3.593 \left(\frac{g_d}{\beta g} \right) \text{ eV} \quad (3.6)$$

For sterile neutrinos produced via the (DW) mechanism, β is adjusted to satisfy this bound with a given mass and $g_d \sim 30$ (although g_d varies rapidly near 150 MeV because of the QCD phase transition or crossover) and for a thermal relic ($\beta = 1$) with $m \sim \text{keV}$ it follows that $g_d \gtrsim 500$, namely such thermal fermion candidate must decouple at a temperature much higher than the electroweak scale.

As discussed in ref.[33] a generalized Tremaine-Gunn[43] bound that yields a *lower* bound on the mass is obtained from the coarse grained primordial phase space density

$$\mathcal{D} = \frac{n(t)}{\langle P_f^2 \rangle} \quad (3.7)$$

where $n(t)$ is the number density of non-relativistic particles and $\langle P_f^2 \rangle$ is the average of the squared physical momentum in the decoupled distribution function. This quantity is a Liouville invariant in absence of gravitational perturbations when the particle has become non-relativistic[33]. The observable quantity is ρ/σ^3 where ρ is the mass density and σ the one dimensional velocity dispersion, therefore we define the primordial phase space density[33]

$$\frac{\rho_{DM}}{\sigma_{DM}^3} = 3^{\frac{3}{2}} m^4 \mathcal{D} = 6.611 \times 10^8 \mathcal{D} \left[\frac{m}{\text{keV}} \right]^4 \frac{M_\odot/\text{kpc}^3}{(\text{km/s})^3}, \quad (3.8)$$

where[33]

$$\mathcal{D} = \frac{g}{2\pi^2} \frac{\left[\int_0^\infty y^2 f_0(y) dy \right]^{\frac{5}{2}}}{\left[\int_0^\infty y^4 f_0(y) dy \right]^{\frac{3}{2}}}. \quad (3.9)$$

The distribution function (2.18) yields

$$\mathcal{D} = \frac{g\Lambda}{2\pi^2} \frac{\left[\frac{3\pi}{2} \zeta(5)\right]^{\frac{5}{2}}}{\left[\frac{105\pi}{8} \zeta(7)\right]^{\frac{3}{2}}} \simeq g\Lambda \times 9.98 \times 10^{-3} \quad (3.10)$$

whereas for fermions that decoupled while relativistic with the generalized distribution (2.2) $\mathcal{D} \sim g\beta \times 1.963 \times 10^{-3}$ [33].

Since the phase space density only diminishes during the merger process (violent relaxation)[43, 51] a lower bound on the mass follows[33],

$$m \geq \frac{[62.36 \text{ eV}]}{\mathcal{D}^{\frac{1}{4}}} \left[10^{-4} \frac{\rho}{\sigma^3} \frac{(\text{km/s})^3}{M_{\odot}/\text{kpc}^3}\right]^{\frac{1}{4}}. \quad (3.11)$$

The compilation of photometric data from (dSphs)[14] yields $[\dots]^{\frac{1}{4}} \sim 1 - 2$, taking the middle of this range as an estimate, the mass of the (DM) particle is bound in the region between the lower bound (3.11) and the upper bound (3.5), namely

$$\frac{316 \text{ eV}}{(g\Lambda)^{\frac{1}{4}}} \leq m \leq 1.33 \left(\frac{\bar{g}}{g\Lambda}\right) \text{ eV} \quad (3.12)$$

Taking as representative values $\bar{g} \sim 100$; $\Lambda \sim 0.05$; $g = 2$ yields

$$560 \text{ eV} \lesssim m \lesssim 1330 \text{ eV} \quad (3.13)$$

constraining the mass in a fairly narrow window within the keV range. A similar conclusion (based on a similar analysis) was obtained in ref.[30].

Thus we see the consistency between the model with scales $\langle\chi\rangle \sim M \sim 100 \text{ GeV}$; $Y \sim 10^{-8}$; $m \sim \text{keV}$ and the constraints from abundance and phase space density of (dSphs).

IV. NON-RELATIVISTIC BOLTZMANN EQUATION: TRANSFER FUNCTION AND POWER SPECTRUM

The transfer function is obtained from the solution of the linearized Boltzmann equation for density and gravitational perturbations. When the particle has become non-relativistic and for wavelengths that are well inside the Hubble radius, the non-relativistic Boltzmann-Vlasov equation describes the evolution of these perturbations. This equation was used in pioneering work on non-relativistic dark matter[54], for neutrinos[23, 39], dark matter perturbations accreted by cosmic strings[55, 56] and more recently to study clustering of thermal relic neutrinos[57]. In all of these previous treatments a numerical analysis was offered but always with a *thermal* distribution function that is truncated to facilitate the numerical integration.

Instead, here we follow the analysis of ref.[47] and implement very accurate analytic approximations for the transfer function that yield a deeper understanding of the connection between the decoupled distribution function and the transfer function, and provide a simple framework to obtain a reliable assessment of the power spectrum for arbitrary range of parameters (mass, coupling, etc) and distribution functions.

To linear order in perturbations the distribution function of the decoupled particle and the Newtonian gravitational potential are[45, 52, 53]

$$f(\vec{p}; \vec{x}; t) = f_0(p) + F_1(\vec{p}; \vec{x}; t) \quad (4.1)$$

$$\varphi(\vec{x}, t) = \varphi_0(\vec{x}, t) + \varphi_1(\vec{x}, t), \quad (4.2)$$

where $f_0(p)$ is the unperturbed distribution function of the decoupled particle, given by (2.18) and for comparison we will also study the generalized distribution (2.2) with $y = p/T_0$, $\varphi_0(\vec{x}, t)$ is the background gravitational potential that determines the homogeneous and isotropic Friedmann-Robertson-Walker metric and \vec{p}, \vec{x} are comoving variables. The reader is referred to refs.[39, 45, 53, 54, 55, 56] for details on the linearization of the collisionless Boltzmann-Vlasov equation.

In conformal time τ and in terms of comoving variables \vec{p}, \vec{x} it is given by[39, 54, 55]

$$\frac{1}{a} \frac{\partial F_1}{\partial \tau} + \frac{\vec{p}}{ma^2} \cdot \vec{\nabla}_{\vec{x}} F_1 - m \vec{\nabla}_{\vec{x}} \varphi_1 \cdot \vec{\nabla}_{\vec{p}} f_0 = 0 \quad (4.3)$$

along with Poisson's equation

$$\nabla_{\vec{x}}^2 \varphi_1 = \frac{4\pi Gm}{a} \int \frac{d^3 p}{(2\pi)^3} F_1(\vec{x}, \tau). \quad (4.4)$$

It is convenient[54, 55] to introduce a new “time” variable s related to conformal time τ by

$$ds = \frac{d\tau}{a}, \quad (4.5)$$

and to take spatial Fourier transforms of $\varphi_1(\vec{x}, \tau)$ and $F_1(\vec{x}, \tau)$ obtaining

$$\frac{\partial F_1(\vec{k}, \vec{p}; s)}{\partial s} + \frac{i\vec{k} \cdot \vec{p}}{m} F_1(\vec{k}, \vec{p}; s) - i\vec{k} \cdot \vec{\nabla}_{\vec{p}} f_0(p) a^2(s) \varphi_1(\vec{k}, s) = 0, \quad (4.6)$$

where

$$\varphi_1(\vec{k}; s) = -\frac{4\pi Gm}{k^2 a(s)} \int \frac{d^3 p}{(2\pi)^3} F_1(\vec{k}, \vec{p}; s). \quad (4.7)$$

The solution of equation (4.6) is

$$F_1(\vec{k}, \vec{p}; s) = F_1(\vec{k}, \vec{p}; s_i) e^{-i\frac{\vec{k} \cdot \vec{p}}{m}(s-s_i)} + im\vec{k} \cdot \vec{\nabla}_{\vec{p}} f_0(p) \int_{s_i}^s ds' e^{-i\frac{\vec{k} \cdot \vec{p}}{m}(s'-s_i)} a^2(s') \varphi_1(\vec{k}, s'). \quad (4.8)$$

The first term on the right hand side is the free-streaming solution in absence of gravitational perturbations. The analysis in ref.[47] shows that $(p/m)(s - s_i)$ is the free streaming distance that the particle travels with comoving velocity p/m from s_i until s . Multiplying both sides of eqn. (4.8) by $-4\pi Gm/[k^2 a(s)]$, integrating in \vec{p} , and using the relation (4.7), we obtain

$$\varphi_1(\vec{k}; s) + i\frac{4\pi Gm^2}{k^2 a(s)} \int \frac{d^3 p}{(2\pi)^3} \vec{k} \cdot \vec{\nabla}_{\vec{p}} f_0(p) \int_{s_i}^s ds' e^{-i\frac{\vec{k} \cdot \vec{p}}{m}(s-s_i)} a^2(s') \varphi_1(\vec{k}, s') = -\frac{4\pi Gm}{k^2 a(s)} \int \frac{d^3 p}{(2\pi)^3} F_1(\vec{k}, \vec{p}; s_i) e^{-i\frac{\vec{k} \cdot \vec{p}}{m}(s-s_i)}. \quad (4.9)$$

The inhomogeneity on the right hand side of this equation is determined by the first term in (4.8) and describes the *free streaming* solution of the Boltzmann-equation in absence of gravitational perturbations.

During matter domination and choosing the initial time at matter-radiation equality $s_i = s_{eq}$, it is found that[47]

$$s - s_{eq} = \frac{2u}{H_{0M} a_{eq}^{\frac{1}{2}}}, \quad (4.10)$$

where

$$H_{0M}^2 = \frac{8\pi G}{3} \rho_{0M} \equiv H_0^2 \Omega_M, \quad (4.11)$$

with $H_0 = 100 h \text{ Kmsec}^{-1} \text{ Mpc}^{-1}$ is the Hubble parameter *today* and ρ_{0M} is the matter density *today*.

Normalizing the scale factor to unity *today*, namely $a(0) = 1$, the variable u is given by[47]

$$u = 1 - \left(\frac{a_{eq}}{a}\right)^{\frac{1}{2}} = 1 - \left[\frac{1+z}{1+z_{eq}}\right]^{\frac{1}{2}}; \quad 0 \leq u \leq 1 - a_{eq}^{\frac{1}{2}}, \quad (4.12)$$

and the scale factor in terms of u is given by

$$a(u) = \frac{a_{eq}}{(1-u)^2}. \quad (4.13)$$

The initial value of the scale factor at matter-radiation equality is $a_{eq} = 1/(1+z_{eq})$ with $z_{eq} \simeq 3050$.

It is convenient to introduce the normalized unperturbed distribution function

$$\tilde{f}_0(y) = \frac{f_0(y)}{\int_0^\infty y^2 f_0(y) dy}, \quad (4.14)$$

which for the non-equilibrium distribution (2.18) is given by

$$\tilde{f}_0(y) = \frac{4}{3\sqrt{\pi}\zeta(5)} \frac{g_{\frac{5}{2}}(y)}{y^{\frac{1}{2}}}. \quad (4.15)$$

Following ref.[47] we introduce the density perturbation normalized at the initial time

$$\delta(\vec{k}, u) = \frac{\int \frac{d^3 p}{(2\pi)^3} F_1(\vec{k}, \vec{p}; s(u))}{\int \frac{d^3 p}{(2\pi)^3} F_1(\vec{k}, \vec{p}; s_{eq})} \quad (4.16)$$

and the gravitational perturbation normalized at the initial time

$$\Phi(\vec{k}, u) = \frac{\varphi_1(\vec{k}, s)}{\varphi_1(\vec{k}, s_{eq})} \quad (4.17)$$

with the relation (see eqn. (4.7))

$$\Phi(\vec{k}; u) = \frac{a_i}{a(u)} \delta(\vec{k}; u) = (1-u)^2 \delta(\vec{k}; u). \quad (4.18)$$

The gravitational perturbation Φ obeys Gilbert's equation[54]

$$\Phi(\vec{k}, u) - \frac{6}{\alpha} (1-u)^2 \int_0^u \Pi[\alpha(u-u')] \frac{\Phi(\vec{k}, u')}{[1-u']^4} du' = (1-u)^2 I[\vec{k}, u]. \quad (4.19)$$

where we have introduced[47]

$$\alpha = \frac{2k \left(\frac{T_0}{m} \right)}{[H_0^2 \Omega_M a_{eq}]^{\frac{1}{2}}} \simeq 1.18 k \times [\text{kpc}] \left(\frac{100}{\bar{g}} \right)^{\frac{1}{3}} \left(\frac{\text{keV}}{m} \right) \sqrt{1+z_{eq}}. \quad (4.20)$$

The non-local kernel is given by

$$\Pi[z] = \int_0^\infty dy y \tilde{f}_0(y) \sin[yz], \quad (4.21)$$

and

$$I[\vec{k}, u] = \frac{\int_0^\infty p^2 dp F_1(\vec{k}, p; s_{eq}) j_0 \left(\frac{\alpha u p}{T_0} \right)}{\int_0^\infty p^2 dp F_1(\vec{k}, p; s_{eq})} \quad (4.22)$$

where $j_0(x) = \sin(x)/x$ and we have assumed that F_1 is a function of $|\vec{p}|$. The inhomogeneity $I[k, u]$ is recognized as the free streaming solution normalized at the initial time, it obeys the initial conditions

$$I[\vec{k}, u=0] = 1 \quad ; \quad \left. \frac{d}{du} I[\vec{k}, u] \right|_{u=0} = 0. \quad (4.23)$$

The density perturbation δ obeys

$$\delta(\vec{k}, u) - \frac{6}{\alpha} \int_0^u \Pi[\alpha(u-u')] \frac{\delta(\vec{k}, u')}{[1-u']^2} du' = I[\vec{k}, u]. \quad (4.24)$$

In ref.[47] it is proven that $\delta \propto a(t)$ as $u \rightarrow 1$, just like fluid density perturbations in a matter dominated cosmology.

As analyzed in ref.[47], the transfer function is obtained from the solution of Gilbert's equation (4.19)[47]. Normalizing it so that $T(k=0) = 1$, it is given by[47]

$$T(k) = \lim_{u \rightarrow 1} \frac{\Phi(\vec{k}, u)}{\Phi(\vec{0}, u)} = \frac{5}{3} \Phi(\vec{k}, u = 1). \quad (4.25)$$

The final power spectrum $P_f(k)$ is related to the initial one $P_i(k)$ as[45]

$$P_f(k) = T^2(k)P_i(k). \quad (4.26)$$

If perturbations do not grow or decay substantially during the prior, radiation dominated phase, $P_i(k)$ is nearly the inflationary primordial power spectrum[45], which is given

$$P_i(k) = A \left(\frac{k}{k_0} \right)^{n_s} \quad (4.27)$$

where the amplitude A and index n_s are determined during inflation and k_0 is a pivot scale. The five years data release from WMAP[58] yields $n_s \approx 0.96$.

Initial conditions: The inhomogeneity $I[\vec{k}, u]$ depends on the initial condition $F_1(\vec{k}, p; s_{eq})$ which must be specified from the evolution of perturbations during the radiation dominated (RD) era up to t_{eq} . During (RD) the Boltzmann equation (4.3) describes the evolution of DM perturbations when the particles are non-relativistic, for the cases under consideration $T \leq m \sim 1$ keV, corresponding to $a \gtrsim 10^{-4} a_{eq}$, and for gravitational perturbations with modes well inside the horizon. During this stage the evolution of the gravitational potential is determined by its coupling to the radiation fluid, it is given by $\varphi_1(k; t) = 3\Phi_p j_1(x)/x$ where Φ_p is the amplitude of primordial perturbations, j_1 is the spherical Bessel function, $x = k\eta/\sqrt{3}$ and η conformal time[45]. $\varphi_1(k; t)$ is strongly suppressed for wavelengths well inside the horizon and can be considered a small perturbation to the evolution of (DM) perturbations[45]. Therefore the evolution of non-relativistic perturbations during (RD) is obtained from the solution (4.8) by neglecting the second term that includes the gravitational potential, namely it is given solely by the free-streaming contribution. Consider an initial condition determined early in the (RD) era at s^* . The free streaming solution of (4.8) during (RD) (neglecting the gravitational potential) is

$$F_1(\vec{k}, \vec{p}; s) = F_1(\vec{k}, \vec{p}; s^*) e^{-i \frac{\vec{k} \cdot \vec{p}}{m} (s - s^*)} \quad ; \quad s - s^* = \frac{\ln \left[\frac{a(s)}{a(s^*)} \right]}{[H_0^2 \Omega_M a_{eq}]^{1/2}}. \quad (4.28)$$

Therefore extrapolating this solution to matter-radiation equality, it follows that the initial condition at t_{eq} , namely $F_1(\vec{k}, \vec{p}; s_{eq})$ is given by (4.28) evaluated at $a(s) = a_{eq}$.

This analysis is akin to the evolution of (CDM) perturbations after decoupling from the radiation fluid studied in ref.[59]. An important difference however, is that sterile neutrinos cannot be described as part of a radiation fluid because they do not interact with radiation, leptons or baryons.

We can now follow all the steps described above leading to eqns. (4.19,4.24) and obtain the same equations but the inhomogeneity $I[k; u]$ replaced by

$$I[k; u] \rightarrow \frac{I[k; u + u_0]}{I[k; u_0]} \quad ; \quad u_0 = \frac{1}{2} \ln \left[\frac{a_{eq}}{a(s^*)} \right] > 0, \quad (4.29)$$

where now

$$I[\vec{k}, u] \equiv \frac{\int_0^\infty p^2 dp F_1(\vec{k}, p; s^*) j_0 \left(\frac{\alpha u p}{T_0} \right)}{\int_0^\infty p^2 dp F_1(\vec{k}, p; s^*)}, \quad (4.30)$$

taking F_1 to be a function of $|\vec{p}|$. It is clear that defining the rescaled perturbations

$$\bar{\Phi}(\vec{k}, u) = \Phi(\vec{k}, u) I[k; u_0] \quad (4.31)$$

$$\bar{\delta}(\vec{k}, u) = \delta(\vec{k}, u) I[k; u_0], \quad (4.32)$$

these obey equations (4.19,4.24) with the inhomogeneity $I[k; u + u_0]$ where $I[k; u]$ is given by (4.30). As it will be shown below $I[k; u_0] < 1$ for $u_0 > 0$. The rescaling of the gravitational and density perturbations by the factor $I[k; u_0]$ reflects the suppression of perturbations by free streaming during the prior (RD) era.

It now remains to determine $F_1(\vec{k}, \vec{p}; s^*)$ to finally obtain $I[k; u]$, here we *assume* adiabatic initial conditions corresponding to a temperature perturbation, namely

$$F_1(\vec{k}, p; s^*) = \left(T \frac{df_0(p, T)}{dT} \right) \left(\frac{\Delta T(\vec{k})}{T} \right). \quad (4.33)$$

These are the initial conditions proposed and studied in refs.[21, 39].

Although a more detailed analysis of the evolution during the radiation era and its impact on the small scale structure will be presented elsewhere, we can obtain an *upper bound* on the small scale properties of the transfer function by setting $u_0 = 0$ ($I[k; 0] = 1$). Furthermore, since our objective is to compare the small scale properties of the transfer function for sterile neutrinos decoupled with the distributions (2.18) and (2.2), it is clear that the distribution (2.18) leads to a *smaller* suppression during (RD) because it favors the small momentum region, therefore yields a smaller free streaming velocity and a smaller free streaming length as compared to the distribution (2.2).

Hence from the above discussion we conclude the following: i) setting $u_0 = 0$ leads to an *upper bound* on $T(k)$, ii) the distribution function (2.2) leads to a *larger* free streaming suppression during (RD) as compared to the case of the distribution function (2.18).

With the distribution function (2.18) and initial condition (4.33) we find that the normalized free streaming solution is given by

$$I[k, u] = \frac{1}{9\sqrt{2}\zeta(5)} \sum_{n=1}^{\infty} \frac{1}{(\rho n)^{\frac{5}{2}}} \left[1 + \frac{n}{\rho} \right]^{\frac{1}{2}} \left\{ \frac{n}{n+\rho} \left[1 + \frac{3}{\rho^2} (n^2 - (\alpha u)^2) \right] + \left[1 + 6 \frac{n^2}{\rho^2} \right] \right\} ; \quad \rho^2 = n^2 + (\alpha u)^2 \quad (4.34)$$

Its asymptotic behavior for $\alpha u \gg 1$ is

$$I[z] \propto z^{-\frac{5}{2}} ; \quad z = \alpha u. \quad (4.35)$$

This power law fall off is strikingly different from that of weakly interacting massive particles (WIMPs) for which the fall-off by free streaming is exponential[47], and that for fermions that decoupled with generalized distributions (2.2) for which the normalized free streaming solution is the same as for a thermal relativistic relic (since the suppression factor β cancels out) and is also a power law but with a *faster* fall off $\propto z^{-4}$, whereas for thermal bosons that decoupled in equilibrium the fall-off is $\propto z^{-2}$ [47]. Thus the non-equilibrium distribution function $f_0(y)$ (2.18) leads to a suppression of the free streaming solution with a power law intermediate between that of thermal ultrarelativistic fermions and bosons. Fig. (3) displays $I[z]; z^{5/2} I[z]$ vs. $z = \alpha u$.

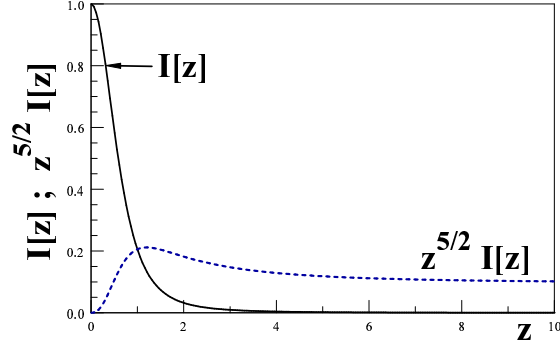


FIG. 3: The free streaming solution $I[z]$ eqn. (4.34) and $z^{\frac{5}{2}} I[z]$ vs. $z = \alpha u$.

It is illustrative to compare the free-streaming solution (4.34) to that of a fermionic species of the same mass that decoupled at the same temperature, therefore has the same α , and initial condition (4.33) but with the generalized distribution (2.2). The free-streaming solution is independent of β and is the same as for a thermal relativistic relic[47]

$$I_{LTE}[k, u] = \frac{2}{9\zeta(3)} \int_0^{\infty} \frac{y^2 e^y}{(e^y + 1)^2} \frac{\sin[y\alpha u]}{\alpha u} dy = \frac{4}{3\zeta(3)} \sum_{n=1}^{\infty} \frac{(-1)^{(n+1)} n}{[n^2 + z^2]^2} \left[1 - \frac{4}{3} \frac{z^2}{[n^2 + z^2]} \right] ; \quad z = \alpha u. \quad (4.36)$$

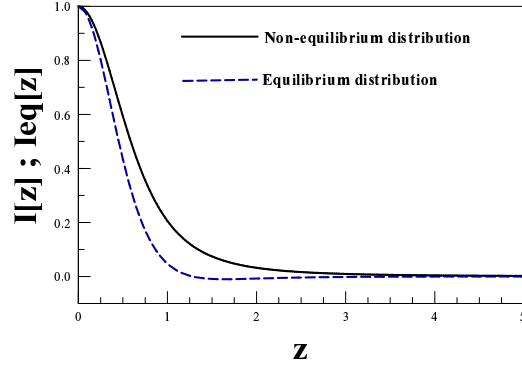


FIG. 4: The free streaming solution $I[z]$ for the non-equilibrium distribution (2.18) eqn. (4.34) (solid line) and for the generalized distribution function eqn. (2.2) (dashed line) vs. $z = \alpha u$.

It is clear that, at least for the initial conditions corresponding to temperature fluctuations (adiabatic) (4.33), the free-streaming solution in absence of gravitational perturbations has a slower fall-off in the case of the non-equilibrium distribution function when compared to the case of the generalized distribution (2.2).

This remarkable difference also emerges in the non-local kernel $\Pi[z]$ in Gilbert's equations for gravitational perturbations(4.19) or for density perturbations (4.24). We find

$$\Pi[z] = \frac{\sqrt{2} z}{\sqrt{3} \zeta(5)} \sum_{n=1}^{\infty} \frac{1}{(\rho n)^{\frac{5}{2}}} \left[1 + \frac{n}{\rho} \right]^{\frac{1}{2}} \left[\frac{2n + \rho}{n + \rho} \right] ; \quad \rho = \sqrt{n^2 + z^2} \quad (4.37)$$

For $z \sim 0$ $\Pi[z] \propto z$ and asymptotically for $z = \alpha(u - u') \gg 1$ we find $\Pi[z] \propto z^{-3/2}$, in contrast with the case of thermal fermions for which the asymptotic behavior is $\Pi[z] \propto z^{-2}$, whereas the asymptotic behavior for thermal bosons is found to be $\Pi[z] \propto z^{-1}$ [47]. Fig.(5) displays $\Pi[z]$ vs. z .

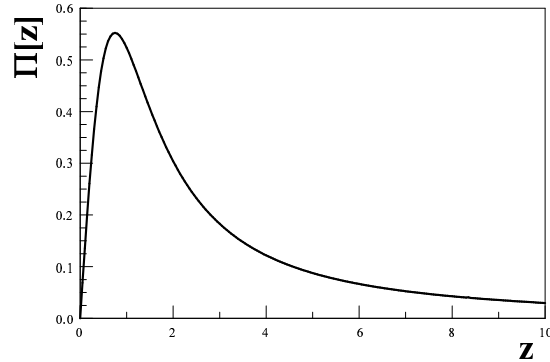


FIG. 5: The kernel $\Pi[z]$ vs. $z = \alpha(u - u')$.

As discussed in detail in ref.[47] the longer range of a kernel leads to an enhancement of the transfer function, and to more power at small scales.

The free streaming wave vector:

The *comoving* free-streaming wave vector is akin to the comoving Jeans wavevector in a fluid but with the speed of sound replaced by the velocity dispersion of the decoupled particle, it is given by

$$k_{fs}(t) = k_{fs}(0) \sqrt{a(t)} \quad (4.38)$$

and its value *today* is[47]

$$k_{fs}(0) = \left[\frac{3H_0^2 \Omega_M}{2 \langle \vec{V}^2 \rangle} \right]^{\frac{1}{2}}, \quad (4.39)$$

where

$$\langle \vec{V}^2 \rangle = \frac{\int d^3p \left(\frac{\vec{p}^2}{m^2} \right) f_0(p)}{\int d^3p f_0(p)} = \left(\frac{T_0}{m} \right)^2 \overline{y^2} \quad (4.40)$$

is the three dimensional velocity dispersion of the non-relativistic particles *today* and we introduced

$$\overline{y^2} = \int_0^\infty dy y^4 \tilde{f}_0(y). \quad (4.41)$$

Using the relation (3.4) and $\Omega_M h^2 = 0.105$ for non-baryonic DM[58], leads to[47]

$$k_{fs}(0) = \frac{0.563}{\sqrt{\overline{y^2}}} \left(\frac{g_d}{2} \right)^{\frac{1}{3}} \left(\frac{m}{\text{keV}} \right) [\text{kpc}]^{-1}. \quad (4.42)$$

The variable α defined in eqn. (4.20) is related to $k_{fs}(t_i)$ as

$$\alpha = \left(\frac{6}{\overline{y^2}} \right)^{\frac{1}{2}} \frac{k}{k_{fs}(t_{eq})}. \quad (4.43)$$

For the non-equilibrium normalized distribution function (4.15) we find

$$\overline{y^2} = \frac{105}{12} \frac{\zeta(7)}{\zeta(5)} \simeq 8.505 \quad (4.44)$$

whereas for the generalized distribution (2.2) is the same as for thermal relativistic fermions,

$$\overline{y^2}|_{LTE} = 15 \frac{\zeta(5)}{\zeta(3)} \simeq 12.939. \quad (4.45)$$

Therefore the *enhancement* of the non-equilibrium distribution function at *small* momenta yields a $\sim 30\%$ reduction in the squared velocity dispersion. Taking the number of relativistic degrees of freedom at decoupling $g_d = \overline{g}$ (see eqn. (2.14) and preceding discussion), we find

$$k_{fs}(0) = 0.193 \left(\frac{\overline{g}}{2} \right)^{\frac{1}{3}} \left(\frac{m}{\text{keV}} \right) [\text{kpc}]^{-1} \simeq 0.711 \left(\frac{\overline{g}}{100} \right)^{\frac{1}{3}} \left(\frac{m}{\text{keV}} \right) [\text{kpc}]^{-1} \quad (4.46)$$

leading to free streaming wavevector and wavelength at matter-radiation equality

$$k_{fs}(t_{eq}) \simeq 0.013 \left(\frac{\overline{g}}{100} \right)^{\frac{1}{3}} \left(\frac{m}{\text{keV}} \right) [\text{kpc}]^{-1} \quad (4.47)$$

$$\lambda_{fs}(t_{eq}) = \frac{2\pi}{k_{fs}(t_{eq})} \simeq 488 \left(\frac{100}{\overline{g}} \right)^{\frac{1}{3}} \left(\frac{\text{keV}}{m} \right) (\text{kpc}). \quad (4.48)$$

For comparison, the value of $k_{fs}(0)$ for a fermion that decoupled with the distribution function (2.2) is the same as for a relativistic thermal fermion, given by [47]

$$k_{fs}^{(dw)}(0) = 0.157 \left(\frac{g_d}{2} \right)^{\frac{1}{3}} \left(\frac{m}{\text{keV}} \right) [\text{kpc}]^{-1}. \quad (4.49)$$

The smaller velocity dispersion in the case of the non-equilibrium distribution function yields a $\sim 30\%$ increase in the free streaming wave vector and consequently a decrease in the free streaming length. But just as importantly in enhancing $k_{fs}(0)$ is decoupling at high temperature for a larger value of g_d .

For comparison, a sterile neutrino produced via the (DW) mechanism $T_d \sim 150 \text{ MeV}; g_d \sim 30$ [24] yields a free streaming wavevector at matter-radiation equality $\lambda_{fs}^{(dw)}(t_{eq}) \sim 900 \text{ kpc}$.

As discussed in ref.[47] an analytic understanding of the transfer function is obtained by rewriting eqn. (4.24) as a differential-integral equation. Taking two derivatives with respect to u and using the original Volterra eqn. (4.24), we obtain

$$\ddot{\delta}(\vec{k}, u) - \frac{6 \delta(\vec{k}, u)}{(1-u)^2} + 3\gamma^2 \delta(\vec{k}, u) - \int_0^u du' K[u-u'] \frac{\delta(\vec{k}, u')}{(1-u')^2} = \ddot{I}[\vec{k}, u] + 3\gamma^2 I[\vec{k}, u], \quad (4.50)$$

where dots refer to derivatives with respect to the variable u and the non-local kernel $K[u-u']$ is given by

$$K[u-u'] = 6\alpha \int_0^\infty y(\overline{y^2} - y^2) \tilde{f}_0(y) \sin[\alpha y(u-u')] dy. \quad (4.51)$$

and γ is defined as

$$3\gamma^2 = \alpha^2 \overline{y^2}. \quad (4.52)$$

From the definitions (4.20) and (4.39) we recognize that the dimensionless ratio

$$\gamma = \frac{\sqrt{2} k}{k_{fs}(t_{eq})}. \quad (4.53)$$

It is convenient to write eqn. (4.50) as

$$\ddot{\delta}(\vec{k}, u) - \frac{6 \delta(\vec{k}, u)}{(1-u)^2} + 3\gamma^2 \delta(\vec{k}, u) = S[\delta; u]. \quad (4.54)$$

The source term is

$$S[\delta; u] = S_0[u] + S_1[\delta; u], \quad (4.55)$$

where

$$S_0[u] = \ddot{I} + 3\gamma^2 I, \quad (4.56)$$

$$S_1[\delta; u] = \int_0^u du' K[u-u'] \frac{\delta(\vec{k}, u')}{[1-u']^2}. \quad (4.57)$$

Passing to cosmic time it is straightforward[47] to find that the left hand side of eqn. (4.54) is precisely of the form of the Jeans equation for fluids but with the adiabatic speed of sound replaced by $\sqrt{\langle \overline{V^2} \rangle}$. However, as discussed in ref.[47] the non-local kernel $K[u-u']$ includes higher order moments of p^2/m^2 than those typically kept in the hierarchy of moment equations[45].

The two terms in the source $S[\delta; u]$ have very different physical interpretations. The first term, S_0 describes a “driving force” resulting from the free streaming of the initial perturbation, the second term S_1 is a *correction* to the fluid description and can be interpreted as a non-local “pressure” term. As discussed in ref.[47] the second term is negligible in the long wavelength limit since $K[u-u'] \propto \alpha^4$ for $\alpha \rightarrow 0$, but becomes important at small scales. Furthermore the *memory* of this kernel is determined by the small- y behavior of the distribution function $\tilde{f}_0(y)$ [47]: larger support at small values of y yields longer range memory kernels, which enhance the transfer function at small scales. This is a consequence of the fact that for kernels with longer range, memory of the initial stages of gravitational clustering persists throughout the evolution leading to a larger contribution to S_1 [47].

The solution of (4.54) can be written exactly in a formal iterative Fredholm series in which the main ingredients are the mode functions corresponding to the fundamental regular and irregular solutions of the homogeneous equation. Defining

$$z = \sqrt{3}\gamma(1-u) \equiv z_0(1-u) \quad ; \quad z_0 = \sqrt{3}\gamma. \quad (4.58)$$

these are

$$h_1(z) = \left(\frac{3}{z^2} - 1 \right) \cos(z) + \frac{3}{z} \sin(z), \quad (4.59)$$

$$h_2(z) = \left(\frac{3}{z^2} - 1 \right) \sin(z) - \frac{3}{z} \cos(z), \quad (4.60)$$

with the following asymptotic behavior as $z \rightarrow 0$ ($u \rightarrow 1$)

$$h_1(z) \rightarrow \frac{3}{z^2} \quad ; \quad h_2(z) \rightarrow \frac{z^3}{15}. \quad (4.61)$$

We emphasize that the kernels $\Pi[z]; K[z]$ *do not depend on the overall normalization of the distribution function*. This is important because Dodelson-Widrow-type distribution functions (2.2) (see also ref.[25]) are of the form

$$f_{dw}(y) = \frac{\beta}{e^y + 1}, \quad (4.62)$$

where $0 \leq \beta \leq 1$ is a *suppression* factor. For these distribution functions the normalized counterpart

$$\tilde{f}_{dw}(y) = \frac{f_{dw}(y)}{\int_0^\infty y^2 f_{dw}(y) dy} = \frac{2}{3\zeta(3)} \frac{1}{e^y + 1} \quad (4.63)$$

is the same as that for a relativistic fermionic thermal relic. The suppression factor β only enters in the abundance and the primordial phase space density. Therefore for sterile neutrinos produced by the (DW) mechanism[24, 25] or for general distribution functions of the form (2.2), the kernels in Gilbert's equation (4.19) or in the equivalent equation (4.50) and the free streaming solution in absence of gravitational perturbations $I[k, u]$ are the *same as for the case of a fermionic relativistic thermal relic*. This results in that the transfer function and power spectrum for sterile neutrinos produced by non-resonant mixing *are the same as that for relativistic thermal fermions* (see below). This observation is relevant in view of the stringent constraints from the analysis in ref.[37]. The results in this reference are based on hydrodynamical simulations that assume a sterile neutrino distribution function of the form (4.62). The overall multiplicative normalization *does not affect the non-local kernel $K[z]$ and as a result, nor does it affect the transfer function and the power spectrum* (see below). This kernel features the asymptotic behavior $\propto 1/z^2$ for any distribution of the form (2.2) as used in ref.[37] for the simulations, whereas for the distribution function (2.18) $K[z] \propto 1/z^{\frac{3}{2}}$. Namely, the kernel falls-off *slower* than in the case of the Dodelson-Widrow production mechanism leading to a longer range of memory of gravitational clustering. The analysis in ref.[47] indicates that this feature, slower fall-off and longer memory range translates in an enhanced transfer function at small scales. This behavior will be confirmed below.

A. The transfer function and power spectrum

From the Fredholm series solution for δ the *exact* transfer function is given by[47]

$$T(k) = \frac{10}{\sqrt{3}\gamma^3} \int_0^1 h_2(u') \left[\frac{I[\vec{k}, u']}{(1-u')^2} + \frac{S_1[\delta; u']}{6} \right] du', \quad (4.64)$$

where δ in S_1 is the Fredholm solution of the integral equation (4.54). As shown in detail in ref.[47] a remarkably accurate approximation to the full transfer function is obtained from the first two terms in the Fredholm series

$$T(k) \simeq T_B(k) + T_{(2)}(k) = \frac{10}{\sqrt{3}\gamma^3} \int_0^1 h_2(u') \left[\frac{I[\vec{k}, u']}{(1-u')^2} + \frac{S_1[\delta^{(1)}; u']}{6} \right] du' \quad (4.65)$$

where the first, Born term is given by

$$T_B(k) = \frac{10}{\sqrt{3}\gamma^3} \int_0^1 h_2(u') \frac{I[\vec{k}, u']}{(1-u')^2} du' \quad (4.66)$$

and the second order correction is given by

$$T_{(2)}(k) = \frac{5}{3\sqrt{3}\gamma^3} \int_0^1 h_2(u') S_1[\delta^{(1)}; u'] du', \quad (4.67)$$

where $\delta^{(1)}(k; u)$ is given by

$$\delta^{(1)}(\vec{k}, u) = I[\vec{k}, u] + \frac{6}{\sqrt{3}\gamma} \int_0^u [h_1(u)h_2(u') - h_2(u)h_1(u')] \frac{I[\vec{k}, u']}{(1-u')^2} du'. \quad (4.68)$$

Since the free streaming solution $I[k; u]$, the kernels and the mode functions are all functions of α (see eqn. (4.20)), it follows that $T(k)$ is a function of α . Therefore it proves convenient to relate the comoving wavelength $\lambda = 2\pi/k$ to α in order to establish the scales that enter in $T(k)$, namely

$$\frac{\lambda}{(\text{kpc})} \simeq \frac{409}{\alpha} \left(\frac{100}{g_d} \right)^{\frac{1}{3}} \left(\frac{\text{keV}}{m} \right) \quad (4.69)$$

where $g_d = \bar{g}$ for sterile neutrinos with the non-equilibrium distribution function (2.18).

The contribution from $T_{(2)}(k)$ is the first correction beyond the fluid approximation and includes the memory of the initial conditions and gravitational clustering. This correction is negligible in the long wavelength limit $\alpha \rightarrow 0$ but becomes important at short scales[47].

Fig. (6) displays the Born term $T_B^2(k)$, the second order corrected $(T_B(k) + T_{(2)}(k))^2$ and the exact $T^2(k)$ obtained from the numerical integration of Gilbert's equation (4.19) with the distribution function (2.18). This figure shows that: (a) the second order correction becomes important at small scales $\alpha > 1$ and (b) that the Born plus second order correction approximation to the transfer function is a remarkably accurate. The outstanding accuracy of the second order approximation was also pointed out in ref.[47] for thermal relics.

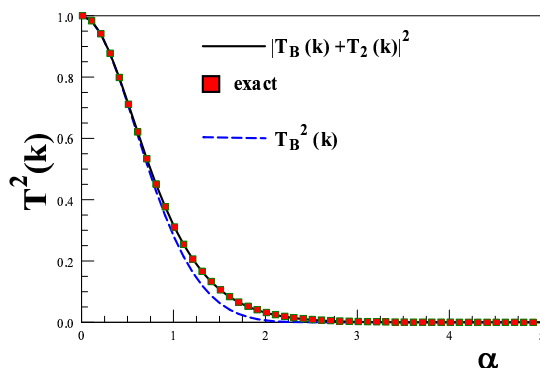


FIG. 6: Comparison between the exact (red squares) solution, the Born approximation and the second order improvement.

Fig. (7) compares $T^2(k)$ for fermions that decoupled with the generalized distribution function (2.2), because the normalized distribution is the same as the case of thermal relativistic relics we refer to this case as *thermal*, and with the non-equilibrium distribution function (2.18) (non-equilibrium). The right panel displays $\ln(T^2(k))$ for both cases to make explicit the *enhancement* of the transfer function for the non-equilibrium case at small scales $\alpha > 1$. There are two different sources of this small scale enhancement: i) the initial condition has a slower fall-off with k in the non-equilibrium case and ii) the kernels $\Pi[z]$ and consequently $K[z]$ also have a slower fall-off with k for large k . Both aspects are a consequence of the enhancement of the distribution function for small y .

Distribution functions that favor the small momentum region yield memory kernels that fall off slower and enhance the transfer function and power spectrum at small scales[47]. This small scale (large α) enhancement is clearly exhibited in the comparison in fig. (7).

Although the simple analytic approximation is easy to study numerically, it is illuminating to provide fitting formulae for $T(k)$ in different ranges of scales. For large scales $k \ll k_{fs}(t_{eq})$ equation (4.50) can be solved in perturbation theory in γ (or α) and the contribution from the non-local kernel K can be neglected to leading order in α , since in the long wavelength limit $K \propto \alpha^4$. In the long-wavelength limit $k \ll k_{fs}(t_{eq})$ we find that $T(k)$ is approximated by

$$T(k) \sim 1 - C \left(\frac{k}{k_{fs}(t_{eq})} \right)^2 + \dots, \quad (4.70)$$

with $C \sim O(1)$ and depends on the distribution function[47]. Of more interest is the small scale behavior for $k \geq k_{fs}(t_{eq})$, because at small scales the contribution from the non-local kernel which is a correction to the *fluid description* that includes memory of gravitational clustering becomes important. Figure (7) shows that $T(k)$ can be approximated by an exponential for $\alpha \gtrsim 0.8$. A numerical analysis yields

$$T(k) \simeq 1.902 e^{-k/k_{fs}(t_{eq})} \quad ; \quad k \geq k_{fs}(t_{eq}), \quad (4.71)$$

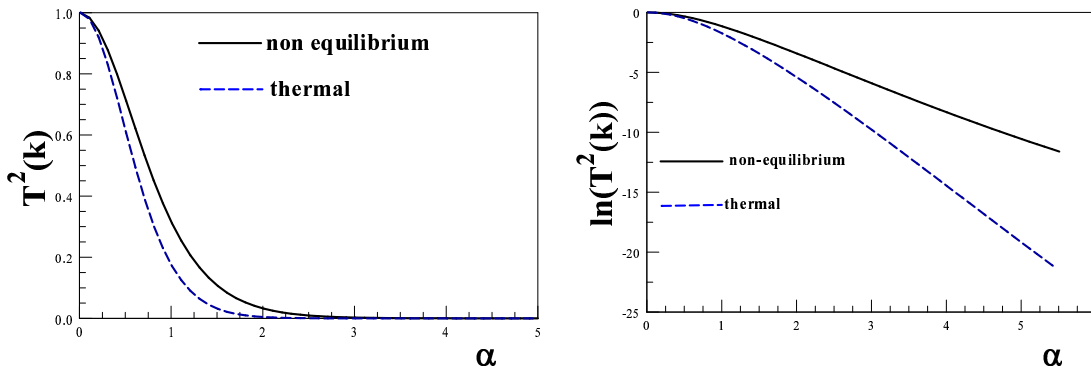


FIG. 7: Left panel: comparison between $T^2(k)$ for thermal fermions and sterile neutrinos decoupled out of equilibrium, right panel: comparison between $\ln(T^2(k))$ for both cases.

in the range $0.8 \lesssim \alpha \leq 6$, where

$$k_{fs}(t_{eq}) \simeq 0.013 \left(\frac{\bar{g}}{100} \right)^{\frac{1}{3}} \left(\frac{m}{\text{keV}} \right) [\text{kpc}]^{-1}. \quad (4.72)$$

The fit (4.70) is better than 2% in this range. For $\bar{g} \sim 100$ and $m \sim 1$ keV the fit (4.71) accurately describes the transfer function in the range

$$65 \text{ kpc} \lesssim \lambda \lesssim 500 \text{ kpc}, \quad (4.73)$$

approximately from the scale of clusters of galaxies to that of galaxies. Within this range $10^{-5} \leq T(k) \leq 0.7$.

The excellent fit (4.71) is different from the often quoted numerical fit by Bardeen *et.al.*[60].

Power spectrum:

Since $T(k)$ is a function of the combination α given by eqn. (4.20) it is convenient to write the power spectrum

$$P(k) = A \left(\frac{k}{k_0} \right)^{n_s} T^2(k) \equiv B \alpha^{n_s} T^2(k). \quad (4.74)$$

Fig. (8) displays $P(k)/B$ vs. α for sterile neutrinos decoupled with (2.2) (equilibrium) and (2.18) (non-equilibrium) as a function of α . The figure reveals that at large scales $\alpha \ll 1$ both feature the same power spectrum (which is the same as that for cold dark matter) but a substantial difference emerges at small scales. The non-equilibrium distribution function (2.18) yields an enhanced transfer function, hence more power at small scales. This is a consequence of the fact that the non-equilibrium distribution function favors smaller values of the momenta (small values of y), leading to smaller velocity dispersion hence *effectively colder* particles, smaller free streaming length, but more importantly a memory kernel of longer range. This feature results in that memory of the gravitational clustering “lingers” longer and the initial value of the gravitational potential influences the process of gravitational clustering during a longer period of time[47] leading to an enhancement of the transfer function and the power spectrum at small scales.

Fig. (7) shows that the suppression scale of $T^2(k)$ for relics that decoupled with (2.2) is at $k \simeq k_{fs}(t_{eq})$. For sterile neutrinos produced via the Dodelson-Widrow mechanism at a temperature $T_d \sim 150$ MeV, with $g_d \sim 30$ and $m = 1$ keV this scale corresponds to a comoving wavelength $\lambda_{fs}^{(dw)}(t_{eq}) \sim 0.9$ Mpc, whereas for a keV sterile neutrino produced in the model under consideration that decoupled with (2.18) with $\bar{g} \sim 100$ this scale corresponds to a comoving wavelength $\lambda_{fs}(t_{eq}) \sim 0.49$ kpc. At smaller scales, for $\alpha \gg 1$ the difference in $T^2(k)$ for thermal relics and the non-equilibrium distribution becomes more dramatic as shown in the right panel of fig.(7).

The small scale enhancement of $T(k)$ is a consequence of the small y behavior of the distribution function, which translates into a longer range kernel $K[z]$. Thus it is clear from these figures that the non-equilibrium distribution function, combined with the higher decoupling temperature, namely the *colder* behavior (smaller velocity dispersion) yield a substantial enhancement of power at small scales as compared to either thermal relics or to sterile neutrinos produced via non-resonant mixing with active neutrinos (namely *a la* Dodelson-Widrow).

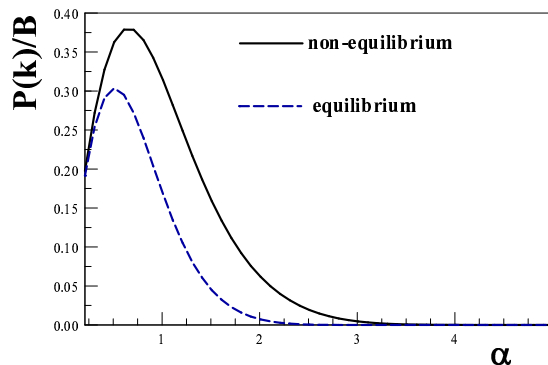


FIG. 8: The spectrum $P(k)/B$ vs. α for the non-equilibrium distribution function (solid line) compared to a thermal fermion relic (dashed line).

For scales $\lambda \gg 1\text{Mpc}$, namely $\alpha \ll 0.4$ the transfer functions and power spectra of sterile neutrinos produced by scalar decay, the (DW) mechanism, relativistic thermal relics or (CDM) are essentially indistinguishable. The non-equilibrium case begins to feature larger power than (DW) and relativistic thermal relics for $\alpha > 0.5$, namely for scales $\lambda \lesssim 0.8\text{Mpc}$ and becomes substantially *larger* than either of these cases for small scales $\lambda \lesssim 490\text{kpc}$.

V. CONCLUSIONS AND FURTHER QUESTIONS

In this article we have implemented a program that begins with the microphysics of production and decoupling of a dark matter particle candidate, constrains the mass and couplings from the observed DM abundance and phase space density of DM dominated satellite galaxies (dSphs) and obtains the DM transfer function and power spectrum by solving the Boltzmann-Vlasov equation for density and gravitational perturbations during matter domination.

The model studied is a phenomenologically appealing extension of the minimal standard model proposed in references[27, 29, 30, 34] in which sterile neutrinos are produced by the decay of a gauge singlet scalar. With the scale of the expectation value and mass of this scalar $\sim 100\text{GeV}$ a consistent description of $\sim \text{keV}$ sterile neutrinos decoupled strongly out of equilibrium at a decoupling temperature $\sim 100\text{GeV}$ emerges and satisfies the DM abundance and phase space constraints from (dSphs).

The distribution function after decoupling for sterile neutrinos produced by gauge singlet decay features a strong enhancement at small comoving momentum $\propto 1/\sqrt{p}$ in contrast to sterile neutrinos produced via non-resonant mixing with active neutrinos (*a la* Dodelson-Widrow) for which the distribution function is that of ultrarelativistic thermal fermions multiplied by a suppression factor. Such distribution function was used in the hydrodynamical simulations performed in ref.[37] to analyze the Lyman- α forest data.

We have implemented an accurate analytic approximation to the solution of the Boltzmann-Vlasov equation and the transfer function introduced in ref.[47] and obtained the power spectrum. This approximation allows to identify which features of the distribution function determine the small scale behavior of the transfer function. Distribution functions that favor small (comoving) momentum lead to longer range memory of gravitational clustering and slower fall-off of the free streaming solution. Both features lead to *small scale enhancement* of the transfer function and power spectrum.

We compare the transfer function and power spectrum in the case of sterile neutrinos produced by gauge singlet decay and by non-resonant mixing with active neutrinos, and find that the former is substantially enhanced over latter at small scales. The transfer function and power spectrum of sterile neutrinos produced via non-resonant mixing is the *same* as that for fermionic thermal relics. The suppression factor in the distribution (see eqn. 2.2) modifies the abundance and primordial phase space densities but *not* the transfer function or power spectrum.

While at large scales $\lambda \gg 1\text{Mpc}$ the transfer function in both cases are nearly indistinguishable and the same as the (CDM) case, the power spectrum for $m \sim \text{keV}$ (DW) sterile neutrinos produced by non-resonant mixing is suppressed below a scale $\lambda \lesssim 900\text{kpc}$ whereas the transfer function for sterile neutrinos produced via scalar decay is suppressed below a scale $\lambda \lesssim 488\text{kpc}$ and substantially enhanced at smaller scales when compared to the (DW) case.

We find the simple fits to $T(k)$ in the limits of large and small scales. For large scales we find

$$T(k) \sim 1 - C \left(\frac{k}{k_{fs}(t_{eq})} \right)^2 + \dots ; \quad k \ll k_{fs}(t_{eq}), \quad (5.1)$$

with $C \sim \mathcal{O}(1)$. In this long wavelength limit the fluid description is valid and the contribution from the memory kernel is subleading.

At small scales the corrections to the fluid description in terms of the non-local kernel that includes memory of gravitational clustering becomes important, in the small scale regime $k \geq k_{fs}(t_{eq})$ a simple and accurate numerical fit yields:

$$T(k) \simeq 1.902 e^{-k/k_{fs}(t_{eq})}, \quad (5.2)$$

where $k_{fs}(t_{eq})$ is the free streaming wave vector at matter-radiation equality. For a sterile neutrino with $m \sim 1$ keV decoupling at $T_d \sim 100$ GeV we find

$$k_{fs}(t_{eq}) \simeq 0.013/\text{kpc}. \quad (5.3)$$

This fit is remarkably accurate in the wide range of scales $60 \text{ kpc} \lesssim \lambda \lesssim 500 \text{ kpc}$ and is different from the often quoted result of ref.[60].

We have given arguments that show that the results presented above are an *upper bound* to the small scale properties of $T(k)$, since the evolution of WDM perturbations during (RD) leads to further suppression of $T(k)$ with a *larger* suppression for the case of sterile neutrinos with distribution functions of the form (2.2) as compared to those with (2.18). This is because the distribution function (2.18) favors the small momentum region leading to shorter free streaming lengths and larger free streaming wavevectors, allowing more power at small scales. A more detailed analysis of the initial conditions obtained by including the evolution during the (RD) will be reported elsewhere.

The substantial difference between the suppression scales in the transfer function and power spectrum at small scales between sterile neutrinos produced by gauge singlet decay and those produced by the (DW) mechanism suggest that sterile neutrinos produced by scalar decay *may* relieve the tension between the constraints from X-ray [35] and Lyman- α forest data[36, 37].

In order to assess whether sterile neutrinos produced by scalar decay may explain the cored profiles of (dSphs), a full N-body simulation with the power spectrum obtained above must be carried out.

Whereas in this article we have focused on the production mechanism from gauge singlet decay, the model includes sterile-active mixing via a see-saw (Majorana) mass matrix. Therefore there is also a complementary mechanism of sterile neutrino production via active-sterile mixing akin to the (DW) mechanism, which is effective at a much lower temperature ~ 150 MeV. The wide separation of decoupling scales, ~ 100 GeV for scalar decay, vs. ~ 150 MeV for (DW) suggests that once the distribution function has been established after decoupling at the higher temperature, the non-equilibrium effects at the lower scale may not modify the small momentum region significantly. We conjecture this to be the case because the wide separation of scales *suggests* that the distribution function obtained from scalar decay, may be taken as an *initial condition* for the kinetics of production via active-sterile mixing, in which case for small mixing angle and neglecting again the build up of the population, the final distribution function would be the *sum* of (2.18) and (2.2).

We have not included this possibility in this article, postponing the more detailed kinetic description, a study of the consequences and different initial conditions to a forthcoming article.

In obtaining the transfer function and power spectrum by solving the Boltzmann-Vlasov equation for (DM) and gravitational perturbations during matter domination, we have neglected the contribution from baryons and photons. Although these will only affect the results for $T(k)$ and $P(k)$ at the few percent level, as discussed in the introduction, a precise assessment of $P(k)$ to few percent accuracy requires solving the full set of Boltzmann-equations by modifying publicly available codes. The study presented in this article provides a reliable preliminary assessment of (DM) candidates, allows a systematic comparison and highlights the important small-scale aspects, perhaps eventually justifying the more numerically demanding task of solving the full set of coupled Boltzmann equations for photons, baryons, gravitational and (DM) perturbations.

Acknowledgments

The author thanks Alex Kusenko for stimulating discussions. He acknowledges support from the U.S. National Science Foundation through grant No: PHY-0553418.

APPENDIX A: THE QUANTUM KINETIC EQUATION

With the Yukawa interaction $\mathcal{L}_I = Y \chi \bar{\nu} \nu$ and χ a scalar field with mass M and ν either a Dirac or Majorana fermion field of mass m the quantum kinetic equation is obtained just as in Minkowski space time by obtaining the total transition probabilities per unit time of the decay and inverse decay processes.

The quantum kinetic equation for the neutrino population $n(p; t)$ (and similarly for the antineutrino) is of the usual form

$$\frac{dn(p; t)}{dt} = \text{Gain} - \text{Loss} \quad (\text{A1})$$

where the gain and loss terms are obtained from the corresponding transition probabilities $|\mathcal{M}_{fi}|^2$. The processes are depicted in fig. (9).

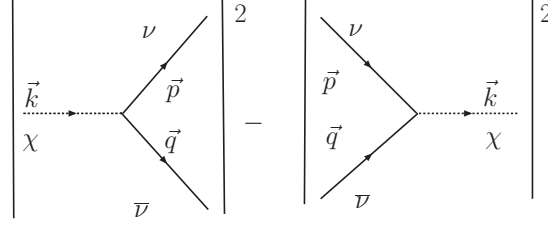


FIG. 9: The “gain” and “loss” contributions to the quantum kinetic equation from the decay $\chi \rightarrow \bar{\nu} \nu$ and inverse decay $\bar{\nu} \nu \rightarrow \chi$, to lowest order in the Yukawa coupling.

The gain term is obtained from the decay reaction $\chi \rightarrow \bar{\nu} \nu$ depicted in the first term in fig. (9) corresponding to an initial state with N_k quanta of the scalar field χ and $n_{p,s}, \bar{n}_{q,s'}$ quanta of neutrinos and antineutrinos respectively with $N_k - 1, n_{p,s} + 1, \bar{n}_{q,s'} + 1$ quanta in the final state respectively. The corresponding Fock states are

$$|i\rangle = |N_k, n_{p,s}, \bar{n}_{q,s'}\rangle \quad ; \quad |f\rangle = |N_k - 1, n_{p,s} + 1, \bar{n}_{q,s'} + 1\rangle \quad (\text{A2})$$

The loss term is obtained from the inverse decay reaction $\bar{\nu} \nu \rightarrow \chi$ corresponding to an initial state with N_k quanta of the scalar field χ and $n_{p,s}, \bar{n}_{q,s'}$ quanta of neutrinos and antineutrinos respectively with $N_k = 1, n_{p,s} - 1, \bar{n}_{q,s'} - 1$ quanta in the final state respectively. The corresponding Fock states are

$$|i\rangle = |N_k, n_{p,s}, \bar{n}_{q,s'}\rangle \quad ; \quad |f\rangle = |N_k + 1, n_{p,s} - 1, \bar{n}_{q,s'} - 1\rangle \quad (\text{A3})$$

The calculation of the matrix elements is standard, the fields are quantized in a volume V in terms of Fock creation-annihilation operators, with the corresponding spinor solutions for the neutrino fields. To lowest order in the Yukawa coupling,

$$\mathcal{M}_{fi} \Big|_{\text{gain}} = -i \frac{Y}{\sqrt{V}} \frac{\delta_{\vec{k}, \vec{p} + \vec{q}}}{\sqrt{2\Omega_k}} \sqrt{N_k} \sqrt{1 - n_p} \sqrt{1 - \bar{n}_q} \bar{U}_\alpha(\vec{p}, s) V_\alpha(\vec{q}, s') (2\pi) \delta(\Omega_k - \omega_p - \omega_q) \quad (\text{A4})$$

similarly, for the loss term we obtain,

$$\mathcal{M}_{fi} \Big|_{\text{loss}} = -i \frac{Y}{\sqrt{V}} \frac{\delta_{\vec{k}, \vec{p} + \vec{q}}}{\sqrt{2\Omega_k}} \sqrt{1 + N_k} \sqrt{n_p} \sqrt{\bar{n}_q} \bar{V}_\alpha(\vec{q}, s') U_\alpha(\vec{p}, s) (2\pi) \delta(\Omega_k - \omega_p - \omega_q) \quad (\text{A5})$$

where the spinors have been normalized to one and the frequencies

$$\Omega_k = \sqrt{k^2 + M^2} \quad ; \quad \omega_p = \sqrt{p^2 + m^2}. \quad (\text{A6})$$

Summing the respective $|\mathcal{M}_{fi}|^2$ over \vec{k}, \vec{q}, s, s' and taking the infinite volume limit we obtain the total transition probability for the gain term

$$\sum_{\vec{k}, \vec{q}, s, s'} |\mathcal{M}_{fi}|^2 \Big|_{\text{gain}} = \text{T} \frac{Y^2}{4\pi} \int d^3q \frac{\delta(\Omega_k - \omega_p - \omega_q)}{\Omega_{\vec{p} + \vec{q}} \omega_p \omega_q} [\omega_p \omega_q - \vec{p} \cdot \vec{q} - m^2] [N_{\vec{p} + \vec{q}} (1 - n_p) (1 - \bar{n}_q)] \quad (\text{A7})$$

where T is the total reaction time. For the loss term we find the same expression but with the replacement $N_{\bar{p}+\bar{q}} \rightarrow 1 + N_{\bar{p}+\bar{q}}$, $(1 - n_p) \rightarrow n_p$, $(1 - \bar{n}_q) \rightarrow \bar{n}_q$. Carrying out the angular integral using the energy-conserving delta function we obtain the final expression for the neutrino production rate

$$\frac{dn(p; t)}{dt} = \frac{1}{T} \left[\sum_{\vec{k}, \vec{q}, s, s'} |\mathcal{M}_{fi}|^2 \Big|_{\text{gain}} - \sum_{\vec{k}, \vec{q}, s, s'} |\mathcal{M}_{fi}|^2 \Big|_{\text{loss}} \right] = \frac{Y^2}{8\pi} \frac{\left(1 - \frac{4m^2}{M^2}\right)}{p\omega_p} \int_{q_-}^{q_+} \frac{qdq}{\omega_q} \left[N_{\bar{p}+\bar{q}}(1-n_p)(1-\bar{n}_q) - (1+N_{\bar{p}+\bar{q}})n_p\bar{n}_q \right] \quad (\text{A8})$$

where q_{\pm} are the roots of the equations

$$\left[(p \pm q_{\pm})^2 + M^2 \right]^{\frac{1}{2}} = \omega_{q_{\pm}} + \omega_p \quad (\text{A9})$$

As discussed in section (II) the relevant limit is $M \gg m$. In this limit $M \gg m$ we find these roots to be

$$q_{\pm} = \frac{M^2}{2m^2} (\omega_p \pm p) \quad (\text{A10})$$

The extension to the cosmological case replaces the momenta by the physical momenta

$$p \rightarrow P_f(t) = \frac{p}{a(t)}, \quad (\text{A11})$$

and for Majorana neutrinos $n = \bar{n}$.

-
- [1] See for example, J. Primack, *New Astron.Rev.* **49**, 25 (2005); arXiv:astro-ph/0609541; in *Formation of structure in the Universe* (Ed. A. Dekel, J. P. Ostriker, Cambridge Univ. Press, Cambridge, 1999) and references therein.
- [2] B. Moore *et al.*, *Astrophys. J. Lett.* **524**, L19 (1999).
- [3] G. Kauffman, S. D. M. White, B. Guiderdoni, *Mon. Not. Roy. Astron. Soc.* **264**, 201 (1993).
- [4] S. Ghigna *et al.* *Astrophys.J.* **544**,616 (2000).
- [5] A. Klypin *et al.* *Astrophys. J.* **523**, 32 (1999); *Astrophys. J.* **522**, 82 (1999).
- [6] B. Willman *et al.* *Mon. Not. Roy. Astron. Soc.* **353**, 639 (2004).
- [7] J. F. Navarro, C. S. Frenk, S. White, *Mon. Not. R. Astron. Soc.* **462**, 563 (1996).
- [8] J. Dubinski, R. Carlberg, *Astrophys.J.* **378**, 496 (1991).
- [9] J. S. Bullock *et al.*, *Mon.Not.Roy.Astron.Soc.* **321**, 559 (2001); A. R. Zentner, J. S. Bullock, *Phys. Rev.* **D66**, 043003 (2002); *Astrophys. J.* **598**, 49 (2003).
- [10] J. Diemand *et al.* *Mon.Not.Roy.Astron.Soc.* **364**, 665 (2005).
- [11] J. J. Dalcanton, C. J. Hogan, *Astrophys. J.* **561**, 35 (2001).
- [12] F. C. van den Bosch, R. A. Swaters, *Mon. Not. Roy. Astron. Soc.* **325**, 1017 (2001).
- [13] R. A. Swaters, *et al.*, *Astrophys. J.* **583**, 732 (2003).
- [14] R. F.G. Wyse and G. Gilmore, arXiv:0708.1492; G. Gilmore *et al.* arXiv:astro-ph/0703308; G. Gilmore *et al.* arXiv:0804.1919 (astro-ph); G. Gilmore, arXiv:astro-ph/0703370.
- [15] G. Gentile *et al.* *Astrophys. J. Lett.* **634**, L145 (2005); G. Gentile *et al.*, *Mon. Not. Roy. Astron. Soc.* **351**, 903 (2004); V.G. J. De Blok *et al.* *Mon. Not. Roy. Astron. Soc.* **340**, 657 (2003), G. Gentile *et al.*, arXiv:astro-ph/0701550; P. Salucci, A. Sinibaldi, *Astron. Astrophys.* **323**, 1 (1997).
- [16] G. Battaglia *et al.* arXiv:0802.4220.
- [19] M. Ryan Joung, R. Cen, G. L. Bryan, arXiv:0805.3150.
- [18] R. Wojtak *et al.* arXiv:0802.0429.
- [19] M.K. Ryan Joung *et al.* arXiv:0805.3150.
- [20] B. Moore, *et al.* *Mon. Not. Roy. Astron. Soc.* **310**, 1147 (1999);
- [21] P. Bode, J. P. Ostriker, N. Turok, *Astrophys. J* **556**, 93 (2001)
- [22] V. Avila-Reese *et al.* *Astrophys. J.* **559**, 516 (2001).
- [23] J. R. Bond, G. Efstathiou, J. Silk, *Phys. Rev. Lett.* **45**, 1980 (1980).
- [24] S. Dodelson, L. M. Widrow, *Phys. Rev. Lett.* **72**, 17 (1994).
- [25] S. Colombi, S. Dodelson, L. M. Widrow, *Astrophys. J.* **458**, 1 (1996).
- [26] X. Shi, G. M. Fuller, *Phys. Rev. Lett.* **82**, 2832 (1999); K. Abazajian, G. M. Fuller, M. Patel, *Phys. Rev.* **D64**, 023501 (2001); K. Abazajian, G. M. Fuller, *Phys. Rev.* **D66**, 023526, (2002); G. M. Fuller *et al.*, *Phys.Rev.* **D68**, 103002 (2003); K. Abazajian, *Phys. Rev.* **D73**,063506 (2006).
- [27] M. Shaposhnikov, I. Tkachev, *Phys. Lett.* **B639**,414 (2006).
- [28] A. Kusenko, arXiv:hep-ph/0703116; arXiv:astro-ph/0608096; T. Asaka, M. Shaposhnikov, A. Kusenko; *Phys.Lett.* **B638**, 401 (2006); P. L. Biermann, A. Kusenko, *Phys. Rev. Lett.* **96**, 091301 (2006).

- [29] K. Petraki, A. Kusenko, Phys. Rev. **D 77**, 065014 (2008).
- [30] K. Petraki, Phys. Rev. **D 77**, 105004 (2008).
- [31] D.F. Mota, V. Pettorino, G. Robbers, C. Wetterich, Phys.Lett.**B663**,160 (2008).
- [32] C. J. Hogan, J. J. Dalcanton, Phys. Rev. **D62**, 063511 (2000).
- [33] D. Boyanovsky, H. J. de Vega, N. Sanchez, Phys. Rev. **D 77**, 043518 (2008).
- [34] A. Kusenko, Phys. Rev. Lett. **97**, 241301 (2006).
- [35] A. Boyarsky *et.al.* Mon. Not. Roy. Astron. Soc. **370**, 213 (2006); Phys. Rev. **D74**, 103506 (2006); A. Boyarski *et. al.* AA, **471**, 51 (2007); Astropart. Phys. **28**, 303 (2007); C. R. Watson *et. al.* Phys. Rev. **D74**, 033009 (2006).
- [36] U. Seljak *et.al.* Phys. Rev. Lett. **97**, 191303 (2006); M. Viel *et.al.* Phys. Rev. Lett. **97**071301 (2006).
- [37] M. Viel *et. al.* , Phys.Rev.Lett. 100 (2008) 041304.
- [38] A. Palazzo *et.al.* arXiv:0707-1495.
- [39] J. R. Bond, A. S. Szalay, Astrophys. J. **274**, 443 (1983).
- [40] E. W. Kolb, M. S. Turner, *The Early Universe* , (Addison-Wesley, Redwood City, CA) (1990).
- [41] D. Boyanovsky, Phys. Rev. **D 77**, 023528 (2008).
- [42] D. Gorbunov, A. Khmelnsky, V. Rubakov, arXiv:0805.2836.
- [43] S. Tremaine, J. E. Gunn, Phys. Rev. Lett. **42**, 407 (1979).
- [44] C.-P. Ma, E. Bertschinger, Astrophys. J. **455**, 7 (1995).
- [45] S. Dodelson *Modern Cosmology*, (Academic Press, N.Y. 2003).
- [46] A. Lewis, A. Challinor, A. Lasenby, Astrophys. J. **538**, 473 (2000).
- [47] D. Boyanovsky, H. J. de Vega, N. Sanchez, arXiv:0807.0622
- [48] D. J. Eisenstein, W. Hu, Astrophys. J. **496**, 605 (1998).
- [49] W. Hu, N. Sugiyama, Astrophys. J. **471**, 542 (1996).
- [50] D. J. Eisenstein *et.al.* Astrophys. J. **633**, 560 (2005).
- [51] D. Lynden-Bell, Mon. Not. Roy. Astron. Soc. **136**, 101 (1967), S. Tremaine, M. Henon, D. Lynden-Bell, Mon. Not. Roy. Astron. Soc. **219**, 285 (1986).
- [52] P. J. E. Peebles, *The Large-Scale Structure of the Universe* (Princeton Series in Physics, Princeton University Press, Princeton, N.J. 1980).
- [53] E. Bertschinger, in *Cosmology and Large Scale Structure*, proceedings, Les Houches Summer School, Session LX, ed. R. Shaeffer *et. al.* (Elsevier, Amsterdam), 273 (1996).
- [54] I. H. Gilbert, Astrophys. J. **144**, 233 (1966); *ibid*, **152**, 1043 (1968).
- [55] R. Brandenberger, N. Kaiser, N. Turok, Phys. Rev. **D36**, 2242 (1987).
- [56] E. Bertschinger, P. N. Watts, Astrophys. J. **328**, 23 (1988).
- [57] A. Ringwald, Y.Y. Y. Wong, JCAP **0412**, 005 (2004); arXiv:hep-ph/0412256.
- [58] E. Komatsu *et. al.* (WMAP collaboration), arXiv:0803.0547.
- [59] A. Loeb, M. Zaldarriaga, Phys. Rev. **D71**, 103520 (2005).
- [60] J. Bardeen *et.al.* Astrophys. J. **304**, 15 (1986).